In vivo formation and repair of DNA double-strand breaks after computed tomography examinations

Markus Löbrich*†, Nicole Rief*, Martin Kühne*, Martina Heckmann‡, Jochen Fleckenstein§, Christian Rübe§, and Michael Uder‡¶

*Fachrichtung Biophysik, ‡Klinik für Diagnostische und Interventionelle Radiologie, and §Klinik für Strahlentherapie und Radioonkologie, Universität des Saarlandes, 66421 Homburg/Saar, Germany; and ¶Institut für Diagnostische Radiologie, Friedrich-Alexander-Universität, 91054 Erlangen, Germany

Edited by Richard B. Setlow, Brookhaven National Laboratory, Upton, NY, and approved May 6, 2005 (received for review March 8, 2005)

Ionizing radiation can lead to a variety of deleterious effects in humans, most importantly to the induction of cancer. DNA double-strand breaks (DSBs) are among the most significant genetic lesions introduced by ionizing radiation that can initiate carcinogenesis. We have enumerated γ-H2AX foci as a measure for DSBs in lymphocytes from individuals undergoing computed tomography examination of the thorax and/or the abdomen. The number of DSBs induced by computed tomography examination was found to depend linearly on the dose–length product, a radiodiagnostic unit that is proportional to both the local dose delivered and the length of the body exposed. Analysis of lymphocytes sampled up to 1 day postirradiation provided kinetics for the *in vivo* loss of γ-H2AX foci that correlated with DSB repair. Interestingly, in contrast to results obtained *in vitro*, normal individuals repair DSBs to background levels. A patient who had previously shown severe side effects after radiotherapy displayed levels of γ-H2AX foci at various sampling times postirradiation that were several times higher than those of normal individuals. γ-H2AX and pulsed-field gel electrophoresis analysis of fibroblasts obtained from this patient confirmed a substantial DSB repair defect. Additionally, these fibroblasts showed significant *in vitro* radiosensitivity. These data show that the *in vivo* induction and repair of DSBs can be assessed in individuals exposed to low radiation doses, adding a further dimension to DSB repair studies and providing the opportunity to identify repair-compromised individuals after diagnostic irradiation procedures.

γ-H2AX foci | ionizing radiation | low radiation doses | radiosensitivity | blood lymphocytes

Ionizing radiation (IR) exposure is frequently encountered in a person's life. Sources of natural radiation include cosmic rays that come from outer space and the sun and radioactive substances that exist in earth and inside the human body. In addition to occupational exposure, flights at high altitude, manned space exploration, and radiological terrorism represent significant sources of radiation risk for part of the population. Diagnostic x-ray procedures including screening tests for cancer are the largest man-made source of radiation exposure, accounting for ≈14% of the total exposure level worldwide (1–4).

Exposure to IR can induce leukemia and other cancers. It is assumed that damage to DNA in the nucleus of a single cell can initiate carcinogenesis. Among the different types of lesions induced, DNA double-strand breaks (DSBs) are considered to be the most relevant of the deleterious effects of IR (5, 6). Remarkably, even a single radiation track and, hence, the smallest possible quantity of IR can produce this kind of damage. Estimates of cancer risk from exposure to IR are based on epidemiological studies of exposed human populations, especially the atomic bomb survivors of Hiroshima and Nagasaki. These studies have provided relatively reliable estimates of risk for moderate to high doses (1, 2). The lowest doses of x-rays or γ-rays for which reasonably reliable evidence of increased cancer risk exists range from 10 to 50 mGy (7). Risk estimates at or below these levels are difficult to obtain directly from epidemiological data (8) and are based, at least partly, on linear extrapolations from existing high-dose data (9–11). However, the validity of this assumption is challenged by some radiobiological phenomena, such as the bystander effect, low-dose hypersensitivity, delayed genomic instability, and induced DNA repair, which are difficult to reconcile with a linear no-threshold hypothesis based on mechanistic considerations (12–17). Because these effects have yet been demonstrated only in cell culture systems or, at best, in animal models, their *in vivo* significance for people has remained unclear. Moreover, many *in vitro* studies involve moderate to high radiation doses, and it is unclear how their findings can be translated into the low-dose range. Hence, there is a clear need to study radiobiological phenomena under *in vivo* conditions after relevant doses of IR.

Recent studies in our laboratory have demonstrated that enumerating γ-H2AX foci (a phosphorylated histone; see refs. 18 and 19) can be used to measure the induction and repair of radiation-induced DSBs in human and mouse cells (17, 20–22). The aim of the present study was to establish γ-H2AX foci formation as an approach to measure the *in vivo* formation and repair of DSBs in individuals. For this, we have enumerated γ-H2AX foci in lymphocytes from individuals undergoing computed tomography (CT) examinations. CT examination was chosen for setting up the γ-H2AX *in vivo* approach because this diagnostic procedure is frequently performed, involves a well defined radiation protocol, and covers a reasonably broad dose range. The analysis of lymphocytes has the advantage that access to the cells is easy and fast and does not require massive medical intervention. Thus, this approach allows the investigation of normal individuals who are exposed to a biologically relevant dose range. Here, we demonstrate the applicability and suitability of γ-H2AX foci analysis as an *in vivo* approach to assess radiation damage and its repair in individuals after low radiation doses.

Materials and Methods

Patients and Irradiation Conditions. Individuals analyzed in this study were examined by CT for benign diseases (13 of 23 individuals) or known malignant neoplasms (10 of 23 individuals). Exclusion criteria were present or past leukemia or lymphoma, radiation therapy within the last 6 months, x-ray examination or scintigraphy within the last 3 days, and age under 18 years. One patient with rectal cancer, HOM-85, received adjuvant radiation therapy (50.4 Gy) to the pelvis 4 years ago and subsequently developed severe side effects (bladder contraction with ureteral stenosis, small bowel necrosis necessitating resec-

This paper was submitted directly (Track II) to the PNAS office.

Freely available online through the PNAS open access option.

Abbreviations: IR, ionizing radiation; CT, computed tomography; DLP, dose–length product; DSB, DNA double-strand break; PFGE, pulsed-field gel electrophoresis; RT, room temperature.

†To whom correspondence should be addressed at: Department of Biophysics, Saarland University, 66421 Homburg/Saar, Germany. E-mail: markus.loebrich@uniklinik-saarland.de.

www.pnas.org/cgi/doi/10.1073/pnas.0501895102

tion, and neural plexus injury causing paraparesis). The study was approved by the ethics committee of the Medical Association of Saarland (Ärztekammer des Saarlandes), and written informed consent was obtained from all patients. MRC-5 (European Collection of Cell Cultures, Porton Down, United Kingdom), HSF1, and HSF2 (provided by K. Dittmann, University of Tübingen, Tübingen, Germany) are primary human fibroblast lines established from normal individuals.

Spiral CT was performed by using a four-detector row scanner (MX8000 IDT, Philips Medical Systems, Eindhoven, The Netherlands) operated at 70–250 mA·s and 120 kV, with a 0.5- to 0.75-s rotation time. The collimation (beam width) varied from 1 to 5 mm, and the pitch, based on the total beam width, varied from 0.5 to 1.25. These parameters provided volumetric CT dose indices ($CTDI_{vol}$) between 4.8 and 17.4 mGy. CT of the thorax was in one phase (with or without contrast media; scan length, 25.3–38.5 cm); CT of the abdomen was performed in two or three phases (upper abdomen including liver, 17–26 cm; optionally upper abdomen contrast enhanced, 17–26 cm; and abdomen and pelvis contrast enhanced, 36.5–53.5 cm); combined thorax/abdomen CT was in three phases (upper abdomen, 22.7–24 cm; thorax and liver contrast enhanced, 33–50.5 cm; abdomen and pelvis contrast enhanced, 43.5–45.5 cm). The dose–length products (DLPs), calculated as the sum of the products of the $CTDI_{vol}$ times the scan length for each phase, ranged from 157 to 1,514 mGy·cm. HOM-85 received a three-phase abdomen CT (scan lengths, 17, 17, and 36.5 cm) with a DLP of 966 mGy·cm. For contrast medium scans, 100–150 ml of iomeprol was injected intravenously (Imeron 300, Bracco ALTANA Pharma, Konstanz, Germany). Incremental CT of the head involved 540 mA·s at 120 kV, 0.5-cm collimation, and 14-cm scan length ($CTDI_{vol}$, 77.2 mGy; DLP, 1,080 mGy·cm). Blood samples were taken from a cubital vein, collected in heparin-containing vials at 37°C, diluted 1:2 with prewarmed RPMI medium 1640 (Biochrom, Berlin) supplemented with 10% FCS and antibiotics, and immediately processed. CT dosimetry was based on measurements made with a Solidose 400 dosimeter with a DCT10 ionization chamber (RTT) according to instructions from Philips.

In vitro x-irradiation was performed at 90 kV, 6 mA, and a dose rate of ≈70 mGy/min with 1 mm of aluminum and 2 mm of plastic between anode and samples. Radiation doses were determined with a PTW-SN4 dosimeter (type 7612) equipped with ionization chamber M23342-751 (7.5–100 kV) or M23331-453 (70 kV to 1 MV) (PTW, Freiburg, Germany) and by using chemical dosimetry, providing a variation range of ≈15%. Diluted blood samples were irradiated in flasks at room temperature (RT). Confluent fibroblasts were irradiated on coverslips in DMEM with 10% FCS and antibiotics at RT. Samples were then incubated for various times in a humidified 5% CO_2 atmosphere at 37°C. Diluted blood samples were cultivated for up to 5 h with minimal changes in background γ-H2AX foci level. For determining DSB induction in lymphocytes, blood samples were diluted, and lymphocytes were separated (see below), cultured in RPMI medium 1640, irradiated at RT, and harvested after a 5-min repair period at 37°C.

Lymphocyte Separation and Immunofluorescence Analysis. Lymphocyte separation was performed according to the manufacturer's instructions (PAA Laboratories, Cölbe, Germany). Briefly, 6-ml diluted blood samples were carefully layered onto 6-ml Ficoll 400 and centrifuged at 1,200 × *g* for 20 min at RT, and lymphocytes from the interphase were washed twice in PBS and spotted onto coverslips for 6 min (or suspended in RPMI medium 1640 for 5-min induction points). This separation yielded ≈80% lymphocytes (60% $CD4^+$, 15% $CD8^+$, and 5% $CD19^+$), ≈15% monocytes, and ≈5% granulocytes (determined by flow cytometry analysis). Monocytes and granulocytes were identified under the microscope by morphological criteria and not included in the analysis. Thus, the data represent a mixture of the different lymphocyte subpopulations.

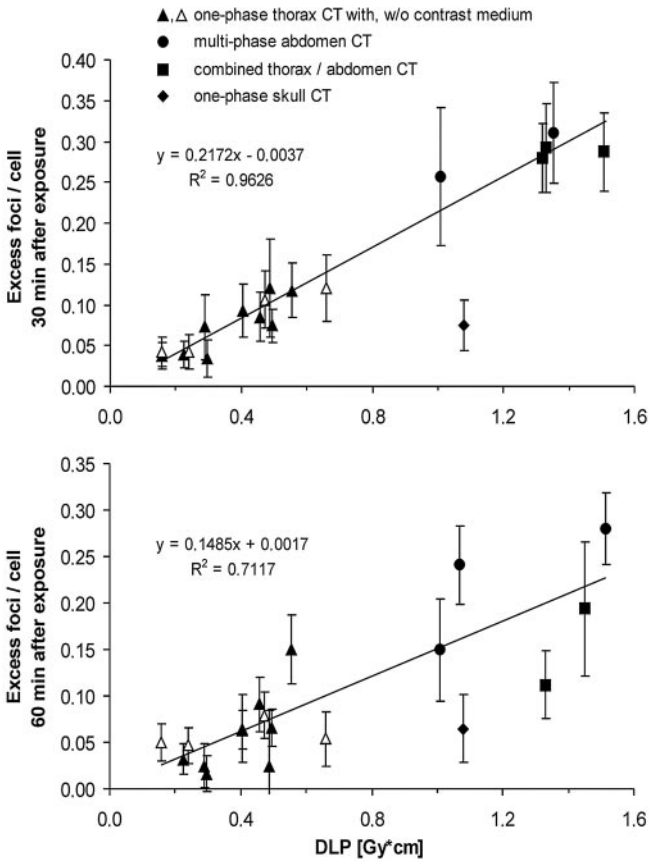

Fig. 1. γ-H2AX foci analysis in lymphocytes from individuals undergoing CT. Blood samples were taken immediately before and at 30 min and/or 60 min after the CT scan; lymphocytes were isolated, fixed, and stained with antibodies against γ-H2AX; and average foci numbers per cell were determined. Shown are excess foci per cell at 30 (*Upper*) and 60 (*Lower*) min for single examinations as a function of the DLP delivered by the CT scan. Lines represent linear fits to all data points except the diamonds; slope, *y* intercept, and fitting quality (R^2) are shown. Background values are similar to those shown in Fig. 2. Error bars represent the SEM.

Fixation for lymphocytes and fibroblasts was for 30 min in 100% methanol and 1 min in 100% acetone at −20°C. Cells were then washed in PBS with 1% FCS for 3 × 10 min at RT. Samples were incubated with anti-γ-H2AX antibody (Upstate, Charlottesville, VA) at a 1:130 dilution for 1 h, washed in PBS with 1% FCS for 3 × 10 min, and incubated with Alexa Fluor 488-conjugated goat anti-mouse secondary antibody (Invitrogen) at a dilution of 1:400 for 1 h, all at RT. Cells were then washed in PBS for 4 × 10 min at RT and mounted by using VECTASHIELD mounting medium with 4′,6-diamidino-2-phenylindole (Vector Laboratories). Fluorescence images were captured by using a Zeiss Axioplan 2 imaging epifluorescent microscope equipped with a charge-coupled device camera and ISIS software (Metasystems, Altlussheim, Germany) and analyzed by eye with a ×63 objective. For each *in vivo* data point, cell counting was performed until, ideally, at least 40 cells and 40 foci were registered; the error bars (Figs. 1 and 2) represent the SEM from the number of cells analyzed; for data points obtained after background subtraction and dose normalization, the SEM was calculated by error propagation. For *in vitro* data points and averaged *in vivo* data, results from different experiments were pooled, and the SEM was calculated as the variation among the single experiments.

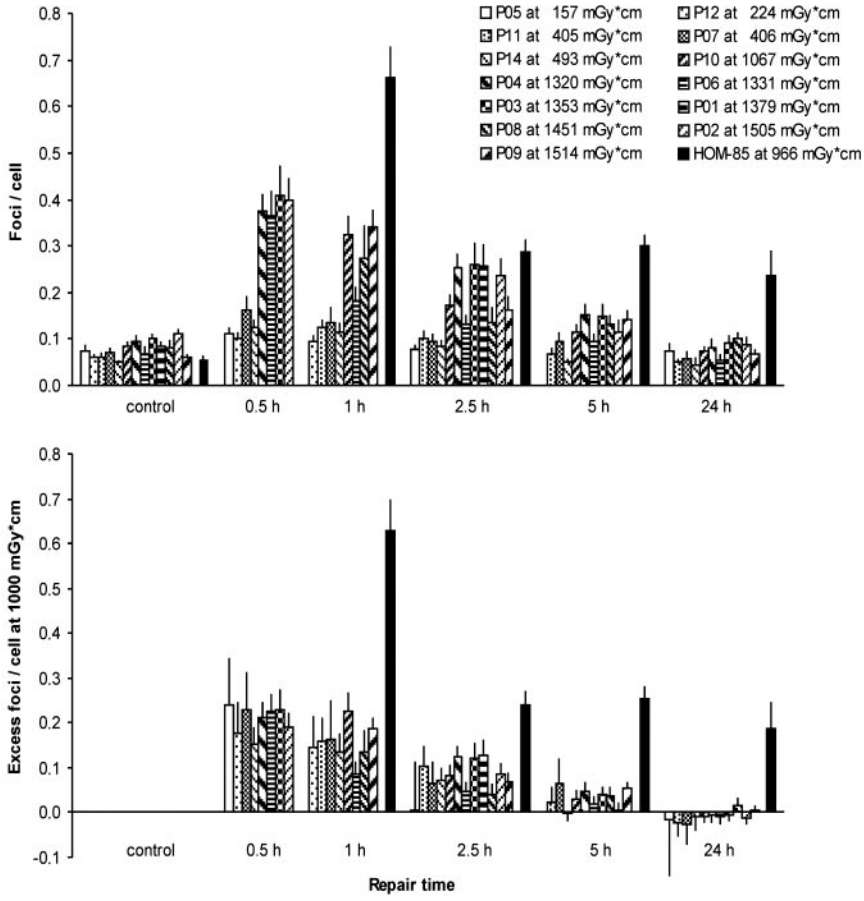

Fig. 2. Kinetics for γ-H2AX foci loss in lymphocytes from individuals after a CT scan. Blood samples were taken immediately before (control) or at the indicated times after CT, and foci numbers were determined. (*Upper*) Data represent the unmodified results for 14 individuals covering a range of DLP values from 150 to 1,500 mGy·cm. (*Lower*) Data were derived by background subtraction and normalization to a DLP of 1,000 mGy·cm. The data at 30 min and 1 h, except those of patient HOM-85, are part of the larger data set shown in Fig. 1. Error bars indicate SEM.

Pulsed-Field Gel Electrophoresis (PFGE) and Radiosensitivity Measurement. PFGE and survival measurements were performed as described in ref. 20. In PFGE experiments, the fraction of DNA entering the gel was quantified and transformed into the percentage of remaining DSBs (23). For survival measurements, cells were irradiated in the confluent state in flasks and plated for colony formation immediately after irradiation. Colonies were stained with crystal violet and counted, typically 4 weeks after irradiation.

Results

***In Vivo* Formation of γ-H2AX Foci.** We investigated the formation of γ-H2AX foci in individuals undergoing CT of the thorax and/or the abdomen. The scans were performed in one, two, or three phases and delivered a DLP (defined as the product of the dose deposited within the exposure field and the length of the body examined) between 150 and 1,500 mGy·cm. In preliminary experiments, blood samples were taken every 10 or 15 min, and foci in lymphocytes were measured. We compared individuals undergoing a one-phase thorax CT (DLP, ≈500 mGy·cm) with those undergoing three-phase thorax/abdomen scans (DLP, ≈1,500 mGy·cm). Up to 30 min after IR, foci numbers either were constant or increased with time; at 30 min, foci numbers were approximately proportional to DLP and decreased thereafter (data not shown). We, therefore, analyzed a series of individuals at 30 and 60 min after CT and observed a linear relationship between the number of γ-H2AX foci and DLP (Fig. 1). The slope and the regression coefficient, R^2, of this relationship were larger at 30 min than at 60 min. The higher foci number at 30 min is consistent with repair occurring between 30 and 60 min; the more pronounced scatter at 60 min may suggest interindividual variations in repair capacity. The linear relationship between foci number and DLP further suggests that one-phase exposures of the thorax (triangles in Fig. 1), multiphase exposures of the abdomen (circles in Fig. 1), and combined thorax/abdomen exposures (squares in Fig. 1) produce similar numbers of foci for the same doses delivered. CT of the head, in contrast, induces significantly fewer foci (diamonds in Fig. 1).

Loss of γ-H2AX Foci in Individuals Reflects Repair of DSBs. We next asked whether the difference in foci level observed between 30 and 60 min after CT reflects repair and whether longer repair times result in further foci loss. To compare individuals examined at different DLPs, the original data obtained up to 24 h after CT were background-subtracted and normalized to a DLP of 1,000 mGy·cm (Fig. 2). Foci loss was seen up to 24 h, at which time all individuals except one (see below for a discussion of this patient) had reached their background value before CT. It is also interesting to note that, notwithstanding some interindividual variation (particularly at repair times ≥1 h), the rate of foci loss among individuals was similar despite the different doses they received (Fig. 2).

The individual *in vivo* kinetics for foci loss at 1,000 mGy·cm were averaged and compared with kinetics obtained after a 20-mGy *in vitro* exposure of fibroblasts (Fig. 3). The comparison with fibroblasts was performed because previous studies had

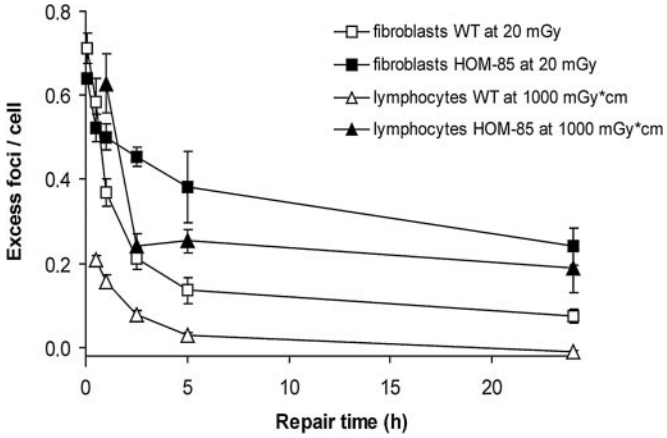

Fig. 3. *In vivo* DSB repair in lymphocytes (triangles) in comparison to *in vitro* DSB repair in fibroblasts (squares). Primary fibroblasts in culture were irradiated *in vitro* with 20 mGy and incubated for 5 min, 30 min, 1 h, 2.5 h, 5 h, and 24 h. Data for WT fibroblasts (open squares) represent the average of the results obtained from MRC-5, HSF1, and HSF2 cells, each analyzed in two independent experiments. Results for patient HOM-85 (filled squares) were obtained in four independent experiments with a fibroblast culture established from this patient. Data for lymphocytes were derived from Fig. 1 (for 30 min and 1 h, calculated as the mean of the normalized data except single-phase skull CT) or Fig. 2 (for 2.5, 5, and 24 h) and represent the average from all normal thorax and/or abdomen patients (WT, open triangles) or the results from patient HOM-85 (filled triangles). Error bars represent the SEM.

shown that in this cell type the loss of IR-induced foci correlates with DSB repair (17, 20–22). Twenty milligrays was chosen because the average damage level in lymphocytes exposed *in vivo* with a DLP of 1,000 mGy·cm is similar to that in lymphocytes irradiated *in vitro* with a dose of ≈20 mGy (see below). Although foci numbers were slightly elevated in fibroblasts at all time points, a similar rate of loss was observed in lymphocytes irradiated *in vivo* compared with fibroblasts irradiated *in vitro*. We, therefore, conclude that the loss of foci in individuals reflects DSB repair.

Lymphocytes from Patients with a DSB Repair Defect Show Elevated Residual Foci After CT. To examine whether the analysis of γ-H2AX foci loss in lymphocytes after CT can detect a DSB repair defect, we analyzed one patient, HOM-85, who had 4 years previously shown exceptionally severe side effects after radiotherapy and who was now undergoing three-phase abdomen CT. Based on clinical radiosensitivity, we reasoned that this patient might carry a DSB repair defect. Remarkably, in this patient at 1, 2.5, and 5 h after CT, we observed levels of residual foci several-fold higher than those observed in the other individuals exposed to the same dose (referred to as "normal individuals") (Fig. 2). Strikingly, at 24 h after CT, a time when normal individuals display background levels of damage, patient HOM-85 exhibited a pronounced level of residual DSBs (Fig. 2). Thus, a clinically radiosensitive patient with a suspected defect in repairing DSBs showed impaired γ-H2AX foci loss after CT.

We next sought to verify the DSB repair defect and, therefore, analyzed fibroblasts obtained from patient HOM-85 after a 20-mGy *in vitro* irradiation by γ-H2AX foci analysis. We observed a repair defect qualitatively and quantitatively similar to the defect obtained in lymphocytes after *in vivo* exposure with 1,000 mGy·cm (Fig. 3). Impaired kinetics for the loss of γ-H2AX foci were also observed after a dose of 2 Gy (data not shown). Fibroblasts from patient HOM-85 were also investigated by PFGE for a repair defect and showed a significant level of unrejoined DSBs for several days postirradiation (Fig. 4*A*). Moreover, significant cellular radiosensitivity (factor of 2) in-

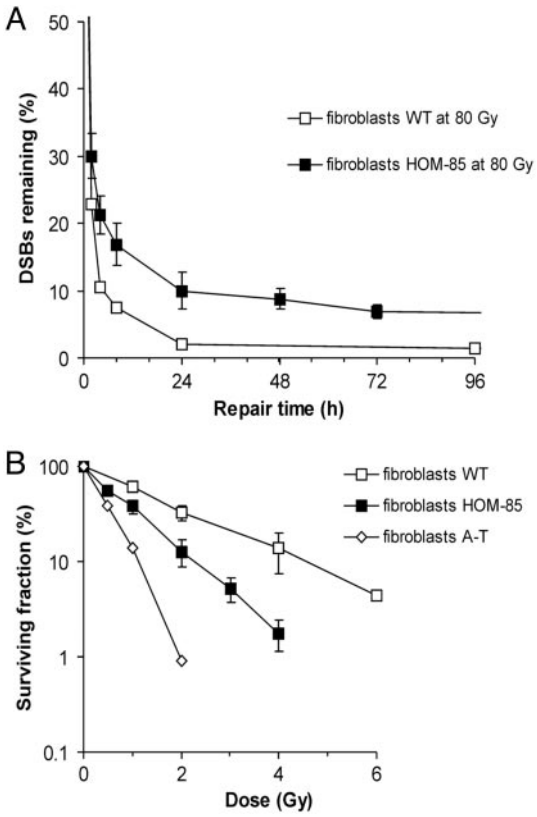

Fig. 4. DSB repair and radiosensitivity in fibroblasts. (*A*) DSB repair in fibroblasts analyzed by PFGE. Confluent fibroblasts were irradiated with 80 Gy, incubated for repair, harvested, and lysed, and the DNA was run on a PFGE gel. The fraction of DNA entering the gel was measured and used to determine the percentage of unrejoined DSBs. Data for WT (open squares) represent the average of results from MRC-5 and HSF1 cells, each analyzed in two independent experiments. Results for patient HOM-85 (filled squares) were obtained in three independent experiments. (*B*) Radiosensitivity of fibroblasts from patient HOM-85 in comparison with the sensitivity of WT fibroblasts and fibroblasts from a patient with ataxia telangiectasia (A-T), a human disorder characterized by extreme radiosensitivity (20). Data for WT (open squares) represent the average of results from MRC-5 and HSF1 cells, each analyzed in two independent experiments. Results for patient HOM-85 (filled squares) were obtained in four independent experiments. Error bars represent the SEM.

dicative of a DSB repair defect was observed in the colony-forming assay (Fig. 4*B*). Together, our results indicate that the clinical radiosensitivity of patient HOM-85 is associated with a marked defect in repairing DSBs that can be detected by γ-H2AX foci analysis in lymphocytes after CT. This substantiates our conclusion that foci loss in individuals represents DSB repair.

Compromised DSB Repair Capacity After *in Vitro* Irradiation of Lymphocytes. We have previously observed that fibroblasts exposed *in vitro* to low radiation doses exhibit a small number of radiation-induced γ-H2AX foci (≈0.05 foci per cell) that persist for several days postirradiation (17). This result is evident in Fig. 3 and has subsequently been confirmed in independent studies (data not shown). To examine whether a similar phenomenon is observed for lymphocytes, we irradiated blood samples *in vitro* with defined doses and analyzed the lymphocytes for γ-H2AX foci at various times after IR (Fig. 5). DSB induction was determined by foci counting at 5 min and found to be linear with dose (≈20 foci per cell per Gy). After repair incubation, the foci levels decreased and showed a nonlinear relationship between

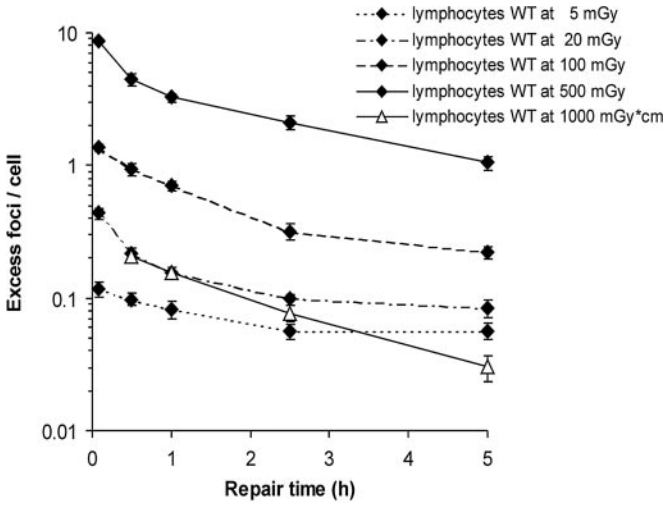

Fig. 5. *In vivo* DSB repair in normal lymphocytes (triangles; taken from Fig. 3) in comparison with *in vitro* DSB repair in normal lymphocytes (diamonds). For *in vitro* kinetics, blood samples were taken, irradiated with 5, 20, 100, or 500 mGy, and incubated for repair for 30 min, 1 h, 2.5 h, or 5 h. Lymphocytes were then isolated and analyzed for γ-H2AX foci. To determine foci numbers at 5 min, isolated lymphocytes were irradiated to avoid repair during the isolation process (see *Materials and Methods*). Foci levels in sham-irradiated cells were constant up to 5 h post-IR (between 0.06 and 0.08 foci per cell). Each data point is the average of four to eight independent determinations. Error bars represent the SEM.

foci number and dose at 5 h post-IR. At this time, foci numbers after a dose of 500 mGy had decreased by almost 90%, whereas only 50% of the foci induced by 5 mGy were lost. This represents a decrease in DSB repair capacity after irradiation with low doses similar to that previously observed *in vitro* with primary human fibroblasts (17). Importantly, this phenomenon is not observed in our *in vivo* repair studies, which show a rate of γ-H2AX foci loss more consistent with that observed *in vitro* after higher doses (Fig. 5).

Discussion

An Approach to Measure DSB Induction and Repair in Individuals Exposed to Low Doses of IR. The validation of γ-H2AX foci analysis in lymphocytes as a sensitive approach to assess the *in vivo* formation and repair of DSBs requires exposure conditions for which reliable dose estimations exist. Ideally, the exposure protocols would cover a substantial dose range, involve highly reproducible irradiation conditions including short exposure times, and be applied to normal individuals. CT examinations of the thorax and/or the abdomen represent such ideal exposure conditions and were applied in the present work to study the *in vivo* formation and repair of γ-H2AX foci. The linear relationship observed between the number of γ-H2AX foci and the DLP of the examination suggests that the amount of damage introduced during CT of the thorax and/or the abdomen is proportional to both the local dose delivered and the length of the body exposed. In contrast, many fewer γ-H2AX foci are formed during CT of the head, consistent with the expectation that a significantly smaller proportion of the blood is exposed during CT of the head. These results strongly suggest that γ-H2AX foci formation can be used to measure the *in vivo* induction of radiation damage after low doses of IR.

By taking blood samples at various times after irradiation, we were able to assess kinetics for the *in vivo* loss of γ-H2AX foci in exposed individuals. Strikingly, the rate of loss of γ-H2AX foci in lymphocytes *in vivo* is similar to that observed when using fibroblasts irradiated *in vitro* (Fig. 3). Because the rate of loss of γ-H2AX foci in fibroblasts has been shown to monitor DSB repair (17, 20–22), this finding strongly suggests that this assay monitors DSB repair *in vivo*. Moreover, a patient displaying severely compromised kinetics for the *in vivo* loss of γ-H2AX foci shows impaired DSB rejoining in fibroblasts analyzed *in vitro* both by γ-H2AX analysis (Fig. 3) and by PFGE (Fig. 4*A*). The latter techniques represent standard fibroblast assays and unambiguously demonstrate the existence of a DSB repair defect in this patient.

To assess the sensitivity of the *in vivo* approach, it is informative to compare the γ-H2AX foci levels after *in vitro* and *in vivo* irradiation. At 30 and 60 min post-IR, the average damage level in lymphocytes from individuals exposed *in vivo* with a DLP of 1,000 mGy·cm is similar to that for lymphocytes irradiated *in vitro* with a dose of ≈20 mGy (Fig. 5). However, the lymphocytes exposed *in vivo* represent a broader range of cells, including those within the exposure field and unexposed cells. In contrast, cells irradiated *in vitro* will have all received the same dose. Because a significant increase in the γ-H2AX foci level could be observed at a DLP as low as 150 mGy·cm (Fig. 1), we suggest that the assay can monitor DSB induction and repair after *in vivo* irradiation with an average dose to the blood of ≈3 mGy.

Individuals Repair IR-Induced DSBs to Background Level. We have previously described that fibroblasts exposed *in vitro* to low radiation doses exhibit a low level of radiation-induced γ-H2AX foci (≈0.05 foci per cell) that persist for several days postirradiation (17). Interestingly, a similar phenomenon is observed after *in vitro* irradiation of lymphocytes, which seem to exhibit a decrease in their repair capacity with decreasing radiation dose (Fig. 5). However, the *in vivo* repair kinetics do not seem to indicate a compromised repair capacity at low radiation doses for the following reasons. First, despite some interindividual differences, the rate of foci loss seems to be dose-independent for DLP values between 150 and 1,500 mGy·cm (corresponding to average lymphocyte doses of 3–30 mGy) (Fig. 2). Second, all normal patients completely lose the radiation-induced DSBs within 24 h, in contrast to a residual foci level (≈0.05 foci per cell) observed at this time in fibroblasts after *in vitro* exposure (Fig. 3). Third, lymphocytes irradiated *in vitro* show dose-dependent repair kinetics that suggest the existence of a residual foci level. However, the *in vivo* foci number at 5 h after a DLP of 1,000 mGy·cm is significantly below the foci level after irradiation with 5 or 20 mGy and more consistent with a dose-independent, complete repair of DSBs (Fig. 5). We cannot rule out the possibility that this difference reflects the distinct irradiation conditions for the *in vitro* and *in vivo* exposures but recognize that it serves as an example for the importance of substantiating *in vitro* findings with *in vivo* data.

γ-H2AX *in Vivo* Analysis as a Predictive Assay for Radiosensitivity. The *in vivo* repair measurements uncovered a DSB repair defect in a person who had previously shown exceptionally severe side effects after radiotherapy (Fig. 2). The repair defect was subsequently confirmed by γ-H2AX and PFGE analysis in a fibroblast culture established from this patient (Figs. 3 and 4*A*). Additionally, the fibroblasts showed significant cellular radiosensitivity (Fig. 4*B*). We conclude that the clinical radiosensitivity of this patient was likely caused by a DSB repair defect. Surprisingly, *in vitro* exposure of lymphocytes from this patient failed to detect the DSB repair defect (unpublished data). This finding cannot presently be explained but is consistent with other studies that failed to observe a correlation between lymphocyte *in vitro* radiosensitivity and the development of adverse radiation reactions (24). Whereas conventional assays designed to evaluate cellular radiosensitivity as a predictor for clinical radiosensitivity typically require labor-intensive procedures over several days or weeks, the *in vivo* γ-H2AX assay is easy, inexpensive, and rapid.

This raises the possibility that cancer patients could be routinely examined for their DSB repair capacity during CT examinations typically performed a few days before radiotherapy.

In summary, we have shown that DSB induction and repair can be assessed in individuals exposed to diagnostic radiation doses. This provides an exciting perspective from which to study DSB repair processes *in vivo* after radiation doses typically encountered in a person's life. The assay's sensitivity and its demonstrated applicability to CT examinations allow the investigation of normal people without clinical symptoms who are exposed to well defined radiation doses. Thus, the assay has the potential to shed light on the *in vivo* significance of some radiobiological phenomena that have hitherto been restricted to *in vitro* measurements, such as the bystander effect (25) or low-dose hypersensitivity (26, 27). Moreover, the assessment of γ-H2AX foci can serve as a biologically relevant biomarker for exposure to low levels of IR. In the clinic, the assay can be applied to biologically determine exposure levels of radiodiagnostic procedures for which physical measurements are difficult to obtain, including, e.g., coronary and cerebral angiography and cardiac catheterization. Finally, the assay could be exploited to optimize radiation doses applied for therapy by predicting an individual's repair capacity.

We thank R. Schepp for excellent technical assistance, K. Rothkamm for methodological contributions at early stages of the project, G. Rhoen for performing flow cytometry characterization of the blood samples, U. Lindemann for biopsy cultivation, J. Berlich and R. Nowack for help with CT dosimetry, H. D. Nagel for valuable comments on CT technology, and P. Jeggo and J. Kiefer for critical comments on the manuscript. This work was supported in part by the Bundesministerium für Bildung und Forschung through the Forschungszentrum Karlsruhe (Grant 02S8132).

1. United Nations Scientific Committee on the Effects of Atomic Radiation (2000) *Sources and Effects of Ionizing Radiation* (United Nations, New York).
2. International Commission on Radiological Protection (1991) *1990 Recommendations of the International Commission on Radiological Protection* (Pergamon, Oxford).
3. Gilbert, E. S. (2001) *Am. J. Epidemiol.* **153,** 319–322.
4. Doll, R. & Wakeford, R. (1997) *Br. J. Radiol.* **70,** 130–139.
5. Burma, S. & Chen, D. J. (2004) *DNA Repair* **3,** 909–918.
6. Dianov, G. L., O'Neill, P. & Goodhead, D. T. (2001) *BioEssays* **23,** 745–749.
7. Brenner, D. J., Doll, R., Goodhead, D. T., Hall, E. J., Land, C. E., Little, J. B., Lubin, J. H., Preston, D. L., Preston, R. J., Puskin, J. S., *et al*. (2003) *Proc. Natl. Acad. Sci. USA* **100,** 13761–13766.
8. Land, C. E. (1980) *Science* **209,** 1197–1203.
9. de Gonzáles, B. A. & Darby, S. (2004) *Lancet* **363,** 345–351.
10. Brenner, D. J. & Elliston, C. D. (2004) *Radiology* **232,** 735–738.
11. Brenner, D. J. (2004) *Radiology* **231,** 440–445.
12. Brenner, D. J. & Sachs, R. K. (2002) *Int. J. Radiat. Biol.* **78,** 593–604.
13. Upton, A. C. (2001) *Crit. Rev. Toxicol.* **31,** 681–695.
14. Nagasawa, H. & Little, J. B. (1999) *Radiat. Res.* **152,** 552–557.
15. Little, J. B. (2000) *Carcinogenesis* **21,** 397–404.
16. Ueno, A. M., Vannais, D. B., Gustafson, D. L., Wong, J. C. & Waldren, C. A. (1996) *Mutat. Res.* **358,** 161–169.
17. Rothkamm, K. & Löbrich, M. (2003) *Proc. Natl. Acad. Sci. USA* **100,** 5057–5062.
18. Rogakou, E. P., Pilch, D. R., Orr, A. H., Ivanova, V. S. & Bonner, W. M. (1998) *J. Biol. Chem.* **273,** 5858–5868.
19. Rogakou, E. P., Boon, C., Redon, C. & Bonner, W. M. (1999) *J. Cell Biol.* **146,** 905–916.
20. Kühne, M., Riballo, E., Rief, N., Rothkamm, K., Jeggo, P. A. & Löbrich, M. (2004) *Cancer Res.* **64,** 500–508.
21. Rothkamm, K., Krüger, I., Thompson, L. H. & Löbrich, M. (2003) *Mol. Cell. Biol.* **23,** 5706–5715.
22. Riballo, E., Kühne, M., Rief, N., Doherty, A., Smith, G. C. M., Recio, M. J., Reis, C., Dahm, K., Fricke, A., Krempler, A., *et al*. (2004) *Mol. Cell* **16,** 715–724.
23. Rothkamm, K. & Löbrich, M. (1999) *Mutat. Res.* **433,** 193–205.
24. Leong, T., Borg, M. & McKay, M. (2004) *Clin. Oncol.* **16,** 206–209.
25. Shao, C., Folkard, M., Michael, B. D. & Prise, K. M. (2004) *Proc. Natl. Acad. Sci. USA* **101,** 13495–13500.
26. Joiner, M. C., Marples, B., Lambin, P., Short, S. C. & Turesson, I. (2001) *Int. J. Radiat. Oncol. Biol. Phys.* **49,** 379–389.
27. Bonner, W. M. (2004) *Mutat. Res.* **568,** 33–39.